# Reactions of Laser-Ablated Fe, Co, and Ni with NO: Infrared Spectra and Density Functional Calculations of $MNO^+$ and $M(NO)_x$ (M = Fe, Co, $x$ = 1−3; M = Ni, $x$ = 1, 2), and $M(NO)_x^-$ (M = Co, Ni; $x$ = 1, 2)

**Mingfei Zhou[†] and Lester Andrews***

*Department of Chemistry, University of Virginia, Charlottesville, Virginia 22904-4319*

*Received: September 17, 1999; In Final Form: December 3, 1999*

Laser-ablated iron, cobalt, and nickel atoms, cations, and electrons have been reacted with NO molecules during condensation in excess neon and argon. The end-on bonded $Fe(NO)_{1-3}$, $Co(NO)_{1-3}$, and $Ni(NO)_{1-2}$ nitrosyls and side-bonded Fe−($\eta^2$-NO), Co−($\eta^2$-NO), and Ni−($\eta^2$-NO) species are formed during sample deposition or on annealing. The $FeNO^+$, $CoNO^+$, and $NiNO^+$ mononitrosyl cations are also produced via metal cation reactions with NO. Evidence is also presented for the $Ni(NO)_{1,2}^-$ and $Co(NO)_{1,2}^-$ anions. The product absorptions are identified by isotopic substitution ($^{15}N^{16}O$, $^{15}N^{18}O$, and mixtures), electron trapping with added $CCl_4$, and density functional calculations of isotopic frequencies. This work provides the first vibrational spectroscopic characterization of Fe, Co, and Ni nitrosyl cations and anions.

## Introduction

The chemistry of nitric oxide with transition metal centers is of great importance in several areas, including surface chemistry, biochemical systems, and especially environmental chemistry. The important interaction of NO with metal surfaces and metal ions on zeolites and metal oxides has been the focus of many extensive studies.[1−11] There are relatively few investigations of NO interacting with bare metal atoms and cations. Thermally evaporated Fe, Co, Ni, Cu, and Zn atom reactions with NO were first studied by Ruschel et al., and iron, cobalt, nickel, and copper nitrosyls were identified using matrix isolation spectroscopy.[12] Recently, infrared spectra of nickel mononitrosyl complexes isolated in solid argon were reinvestigated by Krim et al., who reported convincing evidence for two nickel mononitrosyl complex isomers.[13] In the gas phase, Oriedo and Russell examined the reactivity of NO with $Fe^+$ using ion cyclotron resonance mass spectrometry and concluded that only excited $Fe^+$ reacts with NO.[14] In addition, binding energies of $FeNO^+$, $CoNO^+$, and $Ni(NO)_{1-3}^+$ were determined from a series of ion−molecule reactions.[15,16] Bauschlicher and Bagus reported complete active space (CASSCF) and configuration interaction (CI) calculations on NiNO,[17] and Fenske and Jensen also performed CI calculations on CoNO.[18] More recently, density functional studies of first-row transition metal mononitrosyl neutrals as well as cations,[19,20] the structure and bonding of different [Fe,N,O] isomers,[21] and the bonding of NO to nickel and cobalt clusters have been investigated.[22,23]

Laser-ablated early transition metal atom reactions with NO molecules have been carried out in this laboratory.[24−27] Due to the high reactivity of laser-ablated metal atoms, insertion reactions to form distinct NMO oxide−nitride molecules were observed, while addition reactions to form the end-on bonded nitrosyls and sided-bonded species proceeded on annealing. In this regard, reactions of Fe, Co, and Ni with NO have been reinvestigated using the laser-ablation technique. We will show that besides end-bonded and sided-bonded nitrosyls, mononitrosyl cations and anions are also produced and identified in solid neon.

[†] Permanent address: Laser Chemistry Institute, Fudan University, Shanghai, P.R. China. E-mail: lsa@virginia.edu.

## Experimental Section

The experiment for laser ablation and matrix isolation spectroscopy has been described in detail previously.[24,28] Briefly, the Nd:YAG laser fundamental (1064 nm, 10 Hz repetition rate with 10 ns pulse width) was focused on the rotating metal targets using laser energy ranging from 1 to 20mJ/pulse with lower energies for neon and higher energies for argon matrix investigations. The argon matrix studies employed still lower laser energy and metal concentration than previous studies from this laboratory.[24−27] The present argon matrix experiment used lower metal concentrations than measured by Krim et al.[13] based on the NiNO product yield, and the present argon matrix metal concentrations are therefore estimated to be 0.1%. Metal concentrations in the present neon matrix experiments are an order of magnitude lower and are estimated to be 0.01%. Laser-ablated metal atoms were co-deposited with nitric oxide (0.05−0.5%) in excess argon or neon onto a 10 or 4 K CsI cryogenic window at 2−4 mmol/h for 30 min to 2 h. Nitric oxide (Matheson) and isotopic $^{15}N^{16}O$ and $^{15}N^{18}O$ (Isomet, 99%) and selected mixtures were used in different experiments. FTIR spectra were recorded at 0.5 $cm^{-1}$ resolution on a Nicolet 750 spectrometer with 0.1 $cm^{-1}$ accuracy, using a HgCdTe detector. Matrix samples were annealed at different temperatures, and selected samples were subjected to broadband photolysis by a medium-pressure mercury arc (Philips, 175 W) with the globe removed and glass filters.

## Results

**Infrared Spectra**. Infrared spectra were recorded for laser-ablated iron, cobalt, and nickel co-deposited with NO in neon and argon. Product absorptions are listed in Tables 1−3 and representative spectra are shown in Figures 1−6 with annealing and photolysis behavior. Bands due to NO, $(NO)_2$, $(NO)_2^+$, $(NO)_2^-$, $NO_2$, and $NO_2^-$ are characteristic of laser-ablated metal and neon discharge experiments with NO[24−27,29,30] and are not listed in the tables. Experiments were done with $^{14}N^{16}O$, $^{15}N^{16}O$, $^{15}N^{18}O$, and mixed $^{14}N^{16}O$ + $^{15}N^{16}O$ and $^{15}N^{16}O$ + $^{15}N^{18}O$ samples, and selected spectra are shown in Figures 7−10. Finally, similar experiments were carried out with 0.01% $CCl_4$ added to 0.1% NO in neon to serve as an electron trap.

10.1021/jp993340j CCC: $19.00 
Published on Web 04/04/2000

**TABLE 1: Infrared Absorptions ($cm^{-1}$) from Co-deposition of Laser-Ablated Iron with NO in Excess Neon and Argon**

| | $^{14}N^{16}O$ | $^{15}N^{16}O$ | $^{15}N^{18}O$ | *R*(14/15) | *R*(16/18) | assignment |
|---|---|---|---|---|---|---|
| neon | 1897.3 | 1859.9 | 1816.9 | 1.0201 | 1.0237 | $FeNO^+$ |
| | 1815.5 | 1778.4 | 1740.2 | 1.0209 | 1.0220 | ONFe−($\eta^2$-NO) |
| | 1812.5 | 1775.4 | 1737.4 | 1.0209 | 1.0219 | ONFe−($\eta^2$-NO) |
| | 1810.8 | 1774.0 | 1735.0 | 1.0207 | 1.0225 | $Fe(NO)_2$ |
| | 1766.0 | 1729.6 | 1693.2 | 1.0210 | 1.0215 | FeNO |
| | 1760.7 | 1726.5 | 1685.5 | 1.0198 | 1.0243 | $Fe(NO)_3$ site |
| | 1757.8 | 1723.6 | 1683.2 | 1.0198 | 1.0240 | $Fe(NO)_3$ |
| | 1755.7 | 1721.7 | 1681.2 | 1.0197 | 1.0241 | $Fe(NO)_3$ site |
| | 1744.6 | 1709.4 | 1671.9 | 1.0206 | 1.0224 | $Fe(NO)_2$ |
| | 1671.3 | 1642.8 | | 1.0173 | | $Fe_x(NO)_y$ |
| | 1342.2 | 1320.2 | 1283.2 | 1.0167 | 1.0288 | Fe−($\eta^2$-NO) |
| | 1276.2 | 1254.9 | 1220.1 | 1.0170 | 1.0285 | ONFe−($\eta^2$-NO) |
| | 1274.3 | 1253.0 | 1218.4 | 1.0170 | 1.0284 | ONFe−($\eta^2$-NO) |
| argon | 3579.4 | 3509.2 | 3428.8 | 1.0200 | 1.0234 | $Fe(NO)_3$ |
| | 3503.3 | 3432.2 | 3358.8 | 1.0207 | 1.0219 | $Fe(NO)_2$ |
| | 3475.7 | 3408.2 | 3328.7 | 1.0198 | 1.0239 | $Fe(NO)_3$ |
| | 1799.0 | 1761.5 | 1724.0 | 1.0213 | 1.0218 | ON−Fe−($\eta^2$-NO) |
| | 1798.1 | 1761.5 | 1723.0 | 1.0208 | 1.0223 | $Fe(NO)_2$ |
| | 1794.6 | 1758.3 | | 1.0206 | | $Fe(NO)_3$ |
| | 1748.9 | 1711.9 | 1676.3 | 1.0216 | 1.0212 | FeNO |
| | 1746.9 | | | | | FeNO site |
| | 1742.6 | 1708.8 | 1668.7 | 1.0198 | 1.0240 | $Fe(NO)_3$ |
| | 1731.6 | 1696.3 | 1659.7 | 1.0208 | 1.0221 | $Fe(NO)_2$ |
| | 1667.0 | 1637.7 | 1593.3 | 1.0179 | 1.0279 | $Fe_x(NO)_y$ |
| | 1343.8 | 1321.5 | 1284.8 | 1.0169 | 1.0286 | Fe−($\eta^2$-NO) |
| | 1275.4 | 1252.7 | 1219.2 | 1.0181 | 1.0275 | ON−Fe−($\eta^2$-NO) |
| | 942.7 | 926.8 | 917.0 | 1.0172 | 1.0107 | NFeO? |
| | 920.1 | 920.0 | 876.7 | | 1.0494 | $Fe_xNO$ |
| | 872.8 | 872.8 | 834.5 | | 1.0459 | FeO |
| | 673.8 | 671.3 | 644.0 | 1.0037 | 1.0424 | $Fe_xNO$ |
| | 522.8 | 509.7 | 509.6 | 1.0257 | | $Fe_xNO$ |
| | 513.4 | 499.9 | 495.7 | 1.0270 | 1.0085 | $Fe(NO)_3$ |

**TABLE 2: Infrared Absorptions ($cm^{-1}$) from Co-deposition of Laser-Ablated Co with NO in Excess Neon and Argon**

| | $^{14}N^{16}O$ | $^{15}N^{16}O$ | $^{15}N^{18}O$ | R(14/15) | R(16/18) | assignment |
|---|---|---|---|---|---|---|
| neon | 1957.5 | 1919.0 | 1874.7 | 1.0201 | 1.0236 | $CoNO^+$ |
| | 1912.0 | 1876.0 | 1829.5 | 1.0192 | 1.0254 | $(Co(NO)_3^+$ site) |
| | 1910.7 | 1874.9 | 1828.4 | 1.0191 | 1.0254 | $(Co(NO)_3^+)$ |
| | 1902.7 | 1866.4 | 1821.2 | 1.0194 | 1.0248 | $(Co(NO)_2^+)$ |
| | 1899.5 | 1863.3 | 1818.0 | 1.0194 | 1.0249 | $(Co(NO)_2^+$ site) |
| | 1825.6 | 1789.0 | 1749.7 | 1.0205 | 1.0225 | $Co(NO)_3$ |
| | 1794.2 | 1756.2 | 1720.7 | 1.0216 | 1.0206 | CoNO |
| | 1782.1 | 1744.9 | 1706.6 | 1.0213 | 1.0224 | $Co(NO)_3$ |
| | 1749.1 | 1714.0 | 1676.0 | 1.0205 | 1.0227 | $Co(NO)_2$ |
| | 1732.4 | 1697.3 | 1660.6 | 1.0207 | 1.0221 | $Co_x(NO)_y$ |
| | 1593.8 | 1561.3 | 1527.7 | 1.0208 | 1.0220 | $Co(NO)_2^-$ |
| | 1585.7 | 1554.5 | 1519.0 | 1.0201 | 1.0234 | $CoNO^-$ |
| | 1317.4 | 1295.4 | 1259.5 | 1.0170 | 1.0285 | Co−($\eta^2$-NO) |
| argon | 3630.8 | 3559.3 | 3478.0 | 1.0201 | 1.0234 | $Co(NO)_3$ |
| | 3530.9 | 3461.8 | 3382.4 | 1.0200 | 1.0235 | $Co(NO)_3$ |
| | 3524.8 | 3454.0 | 3378.7 | 1.0205 | 1.0223 | $Co(NO)_2$ |
| | 1846.1 | 1808.3 | 1769.4 | 1.0209 | 1.0220 | OCoNO |
| | 1827.2 | 1790.4 | 1750.6 | 1.0206 | 1.0227 | $Co(NO)_2$ |
| | 1814.6 | 1778.2 | 1738.9 | 1.0205 | 1.0226 | $Co(NO)_3$ |
| | 1770.1 | 1735.4 | 1695.4 | 1.0200 | 1.0236 | $Co(NO)_3$ |
| | 1761.0 | 1724.0 | 1689.3 | 1.0215 | 1.0205 | CoNO |
| | 1737.6 | 1702.6 | 1665.2 | 1.0206 | 1.0225 | $Co(NO)_2$ |
| | 1284.2 | 1262.1 | 1228.6 | 1.0175 | 1.0273 | Co−($\eta^2$-NO) |
| | 822.0 | 821.8 | 787.3 | 1.0002 | 1.0438 | OCoNO |
| | 620.1 | 615.4 | 599.4 | 1.0076 | 1.0267 | CoNO |
| | 581.5 | 577.1 | 565.3 | 1.0076 | 1.0209 | $Co(NO)_2$ |
| | 579.3 | 566.1 | 563.8 | 1.0233 | 1.0041 | $Co(NO)_3$ |
| | 493.8 | 481.7 | 478.8 | 1.0251 | 1.0061 | $Co(NO)_3$ |

**Calculations**. Density functional calculations were performed on metal−NO species using the Gaussian 94 program.[31] The BP86 and B3LYP functionals,[32,33] and the 6-311+G* basis set for N and O atoms, and the Wachters and Hay sets as modified by Gaussian 94 for iron, cobalt, and nickel atoms[34,35] were employed as a guide for vibrational assignments; such calculations have accurately predicted product vibrational frequencies for early transition metal−NO reaction products in this laboratory.[24−27] Geometries were fully optimized and the vibrational frequencies were computed using analytical second derivatives. Calculations were first done on MNO, M−($\eta^2$-NO), $MNO^+$, and $MNO^-$ using both functionals, and the optimized geometries, relative energies, vibrational frequencies, and intensities are listed in Tables 4 and 5. Similar calculations were also done on the $M(NO)_2$ dinitrosyl neutrals, cations, and anions, and the trinitrosyl species using the BP86 functional, and the results are listed in Tables 6 and 7. Figure 11 shows the calculated iron nitrosyl structures.

**TABLE 3: Infrared Absorptions ($cm^{-1}$) from Co-deposition of Laser-Ablated Ni with NO in Excess Neon and Argon**

| | $^{14}N^{16}O$ | $^{15}N^{16}O$ | $^{15}N^{18}O$ | R(14/15) | R(16/18) | assignment |
|---|---|---|---|---|---|---|
| neon | 3572.8 | 3501.1 | 3424.6 | 1.0205 | 1.0223 | $Ni(NO)_2$ |
| | 3337.0 | 3273.3 | 3196.8 | 1.0195 | 1.0239 | NiNO site |
| | 3331.5 | 3268.2 | 3191.2 | 1.0194 | 1.0241 | NiNO |
| | 2001.9 | 1962.5 | 1917.3 | 1.0201 | 1.0236 | $NiNO^+$ |
| | 1926.2 | 1890.4 | 1842.8 | 1.0189 | 1.0258 | $Ni(NO)_2^+$ |
| | 1918.3 | 1882.0 | 1835.7 | 1.0193 | 1.0252 | $(Ni(NO)_3^+)$ |
| | 1916.2 | 1880.0 | 1833.8 | 1.0193 | 1.0252 | $(Ni(NO)_3^+)$ site |
| | 1762.0 | 1726.4 | 1688.9 | 1.0206 | 1.0222 | $Ni(NO)_2$ |
| | 1759.9 | 1724.3 | 1686.8 | 1.0206 | 1.0222 | $Ni(NO)_2$ site |
| | 1682.8 | 1650.5 | 1611.3 | 1.0196 | 1.0243 | NiNO site |
| | 1680.1 | 1647.8 | 1608.6 | 1.0196 | 1.0244 | NiNO |
| | 1665.3 | 1634.9 | 1592.9 | 1.0186 | 1.0264 | $(NO)_xNiNO$ |
| | 1660.4 | 1630.2 | 1588.1 | 1.0185 | 1.0265 | $(NO)_xNiNO$ |
| | 1592.2 | 1559.1 | 1526.9 | 1.0212 | 1.0211 | $Ni(NO)_2^-$ |
| | 1588.9 | 1555.9 | 1524.2 | 1.0212 | 1.0208 | $Ni(NO)_2^-$ site |
| | 1454.7 | 1428.2 | 1392.1 | 1.0186 | 1.0259 | $NiNO^-$ |
| | 1292.6 | 1270.4 | 1236.0 | 1.0175 | 1.0278 | Ni−($\eta^2$-NO) |
| argon | 3555.2 | 3483.9 | 3408.2 | 1.0205 | 1.0222 | $Ni(NO)_2$ |
| | 3323.7 | 3259.1 | 3185.4 | 1.0198 | 1.0231 | NiNO |
| | 1842.0 | 1804.9 | 1764.4 | 1.0206 | 1.0230 | ONiNO |
| | 1813.5 | 1776.3 | 1738.3 | 1.0209 | 1.0219 | $Ni_xNO$ |
| | 1802.6 | 1766.1 | 1727.4 | 1.0207 | 1.0224 | $Ni_xNO$ |
| | 1749.7 | 1714.2 | 1677.2 | 1.0207 | 1.0221 | $Ni(NO)_2$ |
| | 1676.6 | 1643.4 | 1606.3 | 1.0202 | 1.0231 | NiNO |
| | 1651.7 | 1621.5 | 1580.2 | 1.0186 | 1.0261 | $(NO)_x$-NiNO |
| | 1503.8 | 1474.3 | 1440.7 | 1.0200 | 1.0233 | $Ni_xNO$ |
| | 1500.5 | 1470.9 | 1436.7 | 1.0201 | 1.0238 | $Ni_xNO$ |
| | 1293.7 | 1271.3 | 1237.1 | 1.0176 | 1.0276 | Ni−($\eta^2$-NO) |
| | 883.5 | 883.4 | 848.4 | 1.0001 | 1.0413 | $O^{58}NiNO$ |
| | 879.4 | 879.3 | 844.0 | 1.0001 | 1.0418 | $O^{60}NiNO$ |
| | 608.5 | | | | | $^{58}NiNO$ |
| | 605.2 | | | | | $^{60}NiNO$ |
| | 580.9 | 574.6 | 563.7 | 1.0110 | 1.0193 | $x$-$^{58}NiNO$ |
| | 577.9 | 571.7 | 560.5 | 1.0108 | 1.0200 | $x$-$^{60}NiNO$ |
| | 524.4 | 521.8 | 511.2 | 1.0050 | 1.0207 | $^{58}Ni(NO)_2$ |
| | 520.2 | 517.5 | 506.8 | 1.0052 | 1.0211 | $^{60}Ni(NO)_2$ |

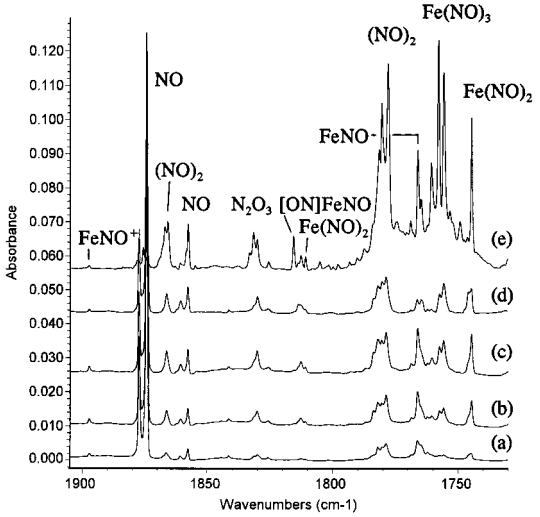


**Figure 1.** Infrared spectra in the 1905−1730 $cm^{-1}$ region from co-deposition of laser-ablated iron with 0.1% NO in neon: (a) after 30 min sample deposition at 4 K, (b) after annealing to 6 K, (c) after annealing to 8 K, (d) after 15 min broadband photolysis, and (e) after annealing to 12 K.

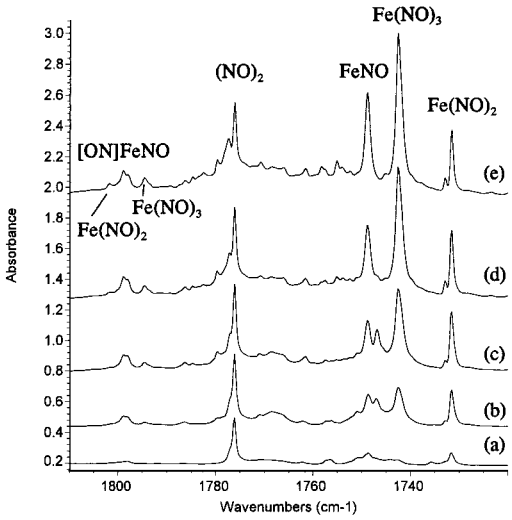


**Figure 2.** Infrared spectra in the 1810−1720 $cm^{-1}$ region from co-deposition of laser-ablated iron with 0.3% NO in argon: (a) after 1 h sample deposition at 10 K, (b) after annealing to 25K, (c) after annealing to 30 K, (d) after annealing to 35 K, and (e) after annealing to 40 K.

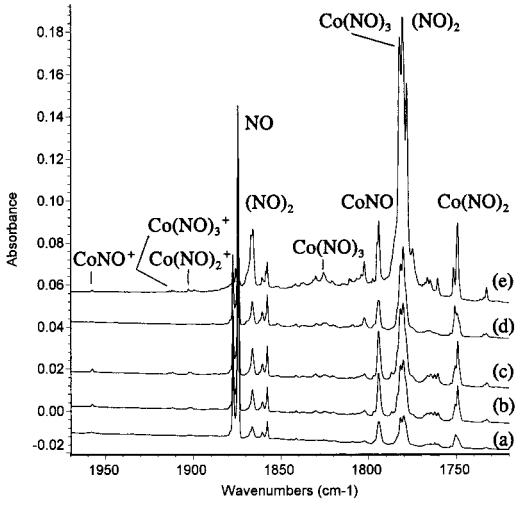


**Figure 3.** Infrared spectra in the 1970−1720 $cm^{-1}$ region from co-deposition of laser-ablated cobalt with 0.1% NO in neon: (a) after 30 min sample deposition at 4 K, (b) after annealing to 6 K, (c) after annealing to 8 K, (d) after 15 min broadband photolysis, and (e) after annealing to 12 K.

## Discussion

**$Fe(NO)_{1-3}$.** Bands at 1748.9, 1731.6, and 1742.6 $cm^{-1}$ in the Fe + NO/Ar system are the major product absorptions in the N−O stretching region. The 1748.9 $cm^{-1}$ band is the strongest after deposition in lower NO concentration experiments, it increases on lower temperature annealing, but less than the 1713.6 and 1742.6 $cm^{-1}$ absorptions on higher temperature annealing. In the mixed $^{14}N^{16}O + {}^{15}N^{16}O$ and $^{15}N^{16}O + {}^{15}N^{18}O$ experiments, only pure isotopic counterparts are present, which confirms the involvement of only one NO subunit. The 1748.9 $cm^{-1}$ band is assigned to FeNO, which is in good agreement with the 1748.7 $cm^{-1}$ argon matrix and 1746.8 $cm^{-1}$ nitrogen matrix bands reported earlier.[12,36] The weak 1731.6 $cm^{-1}$ band after sample deposition increases markedly on lower temperature annealing. In the mixed $^{14}N^{16}O + {}^{15}N^{16}O$ and $^{15}N^{16}O + {}^{15}N^{18}O$ experiments, triplets with approximately 1:2:1 relative intensities are produced, which indicate that two equivalent NO submolecules are involved in this vibration. This band is assigned to the antisymmetric N−O stretching vibration of the $Fe(NO)_2$ molecule, which has been observed at 1731.8 $cm^{-1}$ in the thermal Fe experiments.[12] A weak band at 1798.1 $cm^{-1}$ tracked with the 1731.6 $cm^{-1}$ band, and also exhibited nitrosyl N−O stretching vibrational frequency ratios, and is assigned to the symmetric N−O stretching vibration. A much weaker band at 3503.3 $cm^{-1}$ (1% of 1731.6 $cm^{-1}$) is due to the combination band, which is 26.4 $cm^{-1}$ below the sum of stretching fundamentals and supports their assignment.

The 1742.6 $cm^{-1}$ band only appeared on annealing; it became the strongest band after higher temperature annealing. In the mixed $^{14}N^{16}O + {}^{15}N^{16}O$ experiment, a quartet with approximately 3:1:1:3 relative intensities is observed (Figure 7); this quartet is characteristic of the doubly-degenerate mode of a trigonal species.[37] Accordingly, the 1742.6 $cm^{-1}$ band is assigned to the antisymmetric N−O stretching vibration of the $Fe(NO)_3$ molecule. A weak associated band at 1794.6 $cm^{-1}$ showed a slightly higher 14/15 ratio, and a quartet with approximately 1:3:3:1 relative intensities, which is characteristic of the nondegenerate vibration mode of a trigonal species; hence,

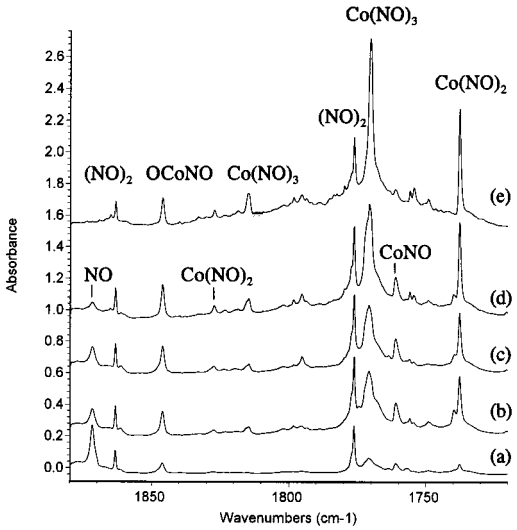


**Figure 4.** Infrared spectra in the 1880−1720 $cm^{-1}$ region from co-deposition of laser-ablated cobalt with 0.3% NO in argon: (a) after 1 h sample deposition at 10 K, (b) after annealing to 25 K, (c) after annealing to 30 K, (d) after annealing to 35 K, and (e) after annealing to 40 K.

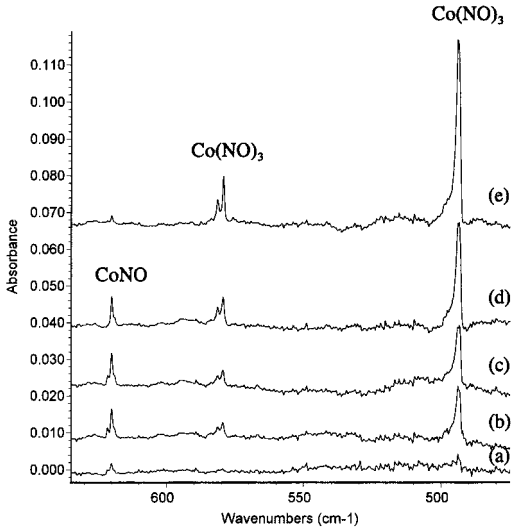


**Figure 5.** Infrared spectra in the 635−475 $cm^{-1}$ region from co-deposition of laser-ablated cobalt with 0.3% NO in argon: (a) after 1 h sample deposition at 10 K, (b) after annealing to 25 K, (c) after annealing to 30 K, (d) after annealing to 35 K, and (e) after annealing to 40 K.

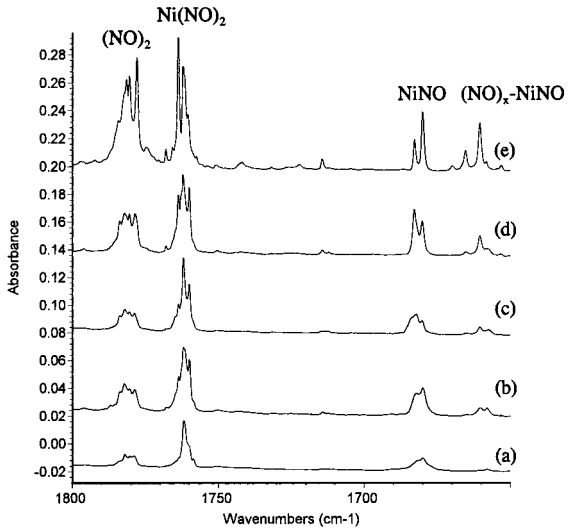


**Figure 6.** Infrared spectra in the 1800−1650 cm$^{-1}$ region from co-deposition of laser-ablated nickel with 0.1% NO in neon: (a) after 30 min sample deposition at 4 K, (b) after annealing to 6 K, (c) after annealing to 8 K, (d) after 15 min broadband photolysis, and (e) after annealing to 12 K.

this band is assigned to the symmetric N−O stretching vibration of the Fe(NO)$_3$ molecule with $C_{3v}$ symmetry. A weak band at 513.4 cm$^{-1}$ exhibited the same annealing and photolysis behavior as the 1742.6 cm$^{-1}$ band; it shifted to 499.9 cm$^{-1}$ with $^{15}N^{16}O$ and to 495.7 cm$^{-1}$ with $^{15}N^{18}O$ and gave a large 14/15 ratio (1.0270) and small 16/18 ratio (1.0085). In the mixed $^{14}N^{16}O + {}^{15}N^{16}O$ experiment, a quartet was also observed. This band is assigned to the antisymmetric Fe−NO stretching vibration of the Fe(NO)$_3$ molecule. Much weaker bands at 3579.4 and 3475.7 cm$^{-1}$ ($A = 0.006$ and 0.005) are due to the overtones of the N−O stretching fundamentals as they are below twice the fundamentals by 9.8 and 9.5 cm$^{-1}$, respectively. The antisymmetric N−O stretching vibrations of FeNO, Fe(NO)$_2$, and Fe(NO)$_3$ are observed at 1766.0, 1744.6, and 1757.8 cm$^{-1}$ in neon, which are blue-shifted 17.1, 13.0, and 15.2 cm$^{-1}$ from the argon matrix band positions. The isotopic frequency ratios in neon are identical to those in argon.

The assignments are strongly supported by DFT calculations. Previous calculations reported a $^2\Delta$ ground state for FeNO;[19,21] our DFT calculations predicted 1785.7 cm$^{-1}$ (BP86) and 1775.7 cm$^{-1}$ (B3LYP) N−O stretching vibrational frequency for the $^2\Delta$ ground state FeNO, which are in good agreement with the observed value. There is no previous report of Fe(NO)$_2$ and Fe(NO)$_3$ calculations; our BP86 calculation predicts a bent $^1A_1$ ground state for Fe(NO)$_2$ with antisymmetric and symmetric N−O stretching vibrations at 1752.4 and 1825.6 cm$^{-1}$. The Fe(NO)$_3$ molecule is calculated to have a $^2A_1$ ground state with $C_{3v}$ symmetry; the antisymmetric and symmetric N−O and antisymmetric Fe−NO stretching vibrations are predicted at 1775.0, 1861.9, and 537.5 cm$^{-1}$, which are in excellent agreement with the observed values.

**Co(NO)$_{1-3}$.** Absorptions at 1761.0 and 620.1 cm$^{-1}$ observed on sample deposition in Co + NO/Ar experiments increased together on lower temperature annealing, and then decreased on higher temperature annealing, giving way to 1737.6 and 1770.1 cm$^{-1}$ absorptions that will be assigned to Co(NO)$_2$ and Co(NO)$_3$ molecules. The 1761.0 cm$^{-1}$ band shows typical nitrosyl N−O stretching isotopic ratios (1.0215 for 14/15; 1.0205 for 16/18), while the 620.1 cm$^{-1}$ band exhibits isotopic ratios of 1.0076 for 14/15 and 1.0267 for 16/18. Although the mixed isotopic structure for the 1761.0 cm$^{-1}$ band is not clear due to band overlap in this region, a clear doublet is observed for the 620.1 cm$^{-1}$ band, which confirms that only one NO submolecule is involved. Ruschel et al.[12] assigned a 1767.2 cm$^{-1}$ band to CoNO and a 1760.6 cm$^{-1}$ band to the Co$_2$NO molecule in their argon matrix. However, there is no 1767 cm$^{-1}$ band observed in our experiments, and the preferential growth of strong Co(NO)$_2$ and Co(NO)$_3$ absorptions at the expense of the 1761.0 cm$^{-1}$ absorption suggests a single Co atom in this product. The 1761.0 and 620.1 cm$^{-1}$ bands are assigned here to the CoNO molecule. Note that no Co(NO)$_3$ absorptions were observed in the thermal Co experiments;[12] this shows that the Co concentrations are relatively high and metal cluster species dominate. In spite of the fact that Co tends to dimerize in the absence of other reagents, the present observation of Co(NO)$_3$ demonstrates that the Co/NO ratio is substantially less in the present laser-ablation experiments than in the previous thermal experiments.[12]

Previous DFT calculations predicted the CoNO molecule to have a triplet ground state with bent geometry.[12,19] Although our B3LYP calculation finds the $^3A''$ state lower in energy, the calculated N−O and Co−NO stretching frequencies are too low to fit the experimental values; however, our BP86 calculation predicted the linear $^1\Sigma^+$ state more stable than the triplet state and N−O and Co−NO stretching vibrational frequencies at 1832.0 and 704.5 cm$^{-1}$. Of at least equal importance, the calculated isotopic frequency ratios (14/15: 1.0225, 1.0067; 16/18: 1.0202, 1.0284) fit the experimental values much better than the triplet state isotopic frequency ratios. All of these strongly suggest a linear $^1\Sigma^+$ ground state for the CoNO molecule. Note that both the isoelectronic NiCO[38] and NiNO$^+$ species have $^1\Sigma^+$ ground states. The CoNO molecule was observed at 1794.2 cm$^{-1}$ in solid neon with almost the same isotopic ratios as the argon matrix frequencies.

Ruschel et al.[12] assigned a 1794.6 cm$^{-1}$ band to the Co(NO)$_2$ molecule, and two bands at 1737.1 and 1846.2 cm$^{-1}$ to Co$_2$(NO)$_2$ molecules without benefit of isotopically mixed precursors. In our experiments, a weak absorption is observed at 1795 cm$^{-1}$ only after annealing, so this must be due to an aggregate species. Our 1846.1 cm$^{-1}$ band tracks with an 822.0 cm$^{-1}$ absorption and will be assigned below to OCoNO. However, a sharp band at 1737.6 cm$^{-1}$ increased markedly on annealing, and a *clear triplet* with approximately 1:2:1 relative intensities was observed in the mixed $^{14}N^{16}O + {}^{15}N^{16}O$ experiments (Figure 8), which is appropriate for the antisymmetric N−O stretching vibration of the Co(NO)$_2$ molecule *with two equivalent NO subunits*. A weak band at 1827.2 cm$^{-1}$ tracked with the 1737.6 cm$^{-1}$ band and is assigned to the symmetric N−O stretching vibration mode. The combination band ($A = 0.007$) was observed at 3524.8 cm$^{-1}$, which is 40.0 cm$^{-1}$ below the sum of fundamentals and supports their assignments. The antisymmetric N−O stretching vibration of the Co(NO)$_2$ molecule is observed at 1749.1 cm$^{-1}$ in neon, and no obvious band can be assigned to the symmetric N−O stretching vibration, suggesting that Co(NO)$_2$ has linear or near linear geometry in neon. Our BP86 calculation predicted a $^2B_1$ ground state for Co(NO)$_2$ with antisymmetric and symmetric N−O stretching vibrations at 1767.3 and 1836.7 cm$^{-1}$. The weight of evidence with both symmetric and antisymmetric N−O stretching fundamentals and their combination band confirms the present new assignment and spectroscopic identification of Co(NO)$_2$.

Four bands at 1814.6, 1770.1, 579.3, and 493.8 cm$^{-1}$ increased together on annealing in solid argon (Figures 4 and 5). The two upper bands exhibited N−O stretching frequency ratios. The two lower bands showed large 14/15 ratios (1.0233 and 1.0251) and small 16/18 ratios (1.0041 and 1.0061),

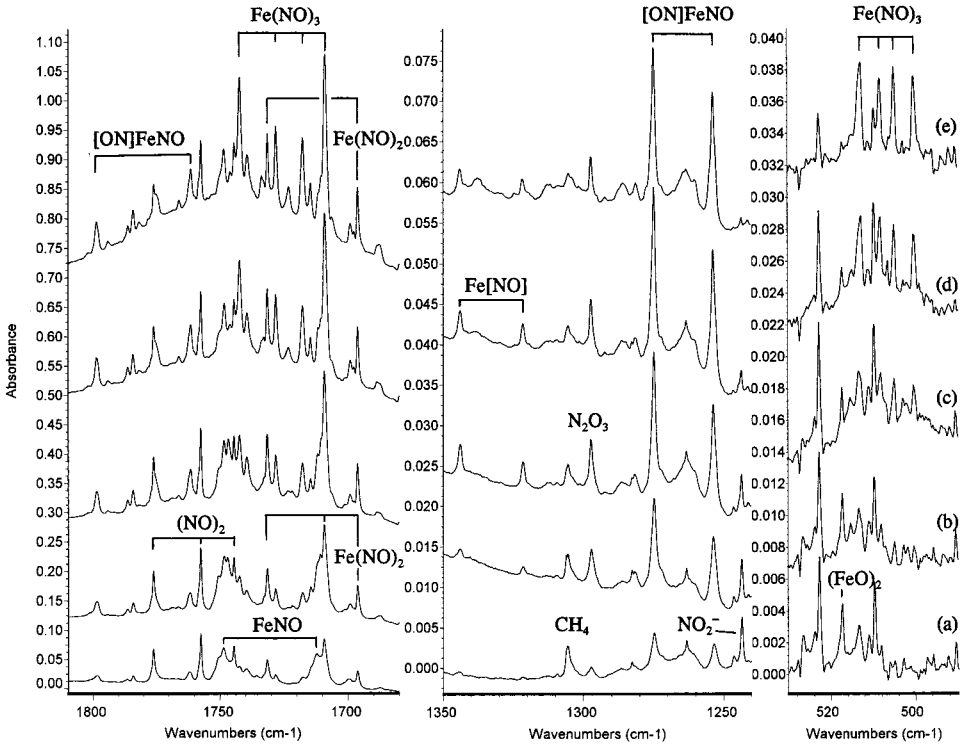


**Figure 7.** Infrared spectra in the 1810−1680, 1350−1240, and 530−490 $cm^{-1}$ regions from co-deposition of laser-ablated iron with 0.15% $^{14}N^{16}O$ + 0.15% $^{15}N^{16}O$ in argon: (a) after 1 h sample deposition at 10 K, (b) after annealing to 25 K, (c) after annealing to 30 K, (d) after annealing to 35 K, and (e) after annealing to 40 K.

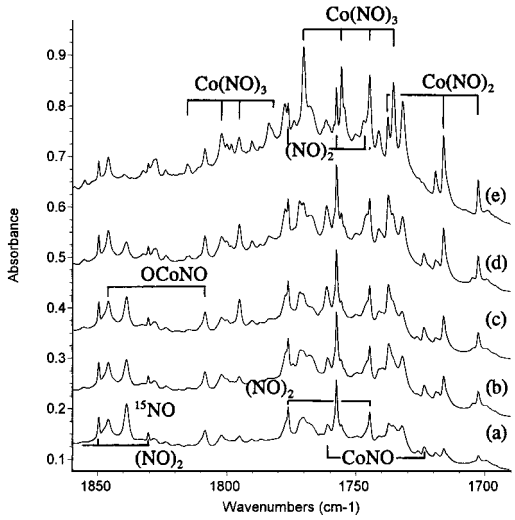


**Figure 8.** Infrared spectra in the 1860−1690 $cm^{-1}$ region from co-deposition of laser-ablated cobalt with 0.15% $^{14}N^{16}O$ + 0.15% $^{15}N^{16}O$ in argon: (a) after 1 h sample deposition at 10 K, (b) after annealing to 25 K, (c) after annealing to 30 K, (d) after annealing to 35 K, and (e) after annealing to 40 K.

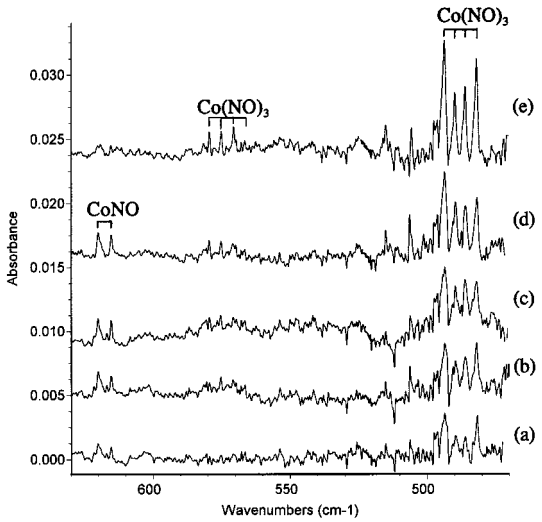


**Figure 9.** Infrared spectra in the 630−470 $cm^{-1}$ region from co-deposition of laser-ablated cobalt with 0.15% $^{14}N^{16}O$ + 0.15% $^{15}N^{16}O$ in argon: (a) after 1 h sample deposition at 10 K, (b) after annealing to 25 K, (c) after annealing to 30 K, (d) after annealing to 35 K, and (e) after annealing to 40 K.

indicating that these two bands belong to Co−NO stretching vibrations. In the mixed $^{14}N^{16}O$ + $^{15}N^{16}O$ experiment, clear quartets were observed for the 1770.1, 579.3, and 493.8 $cm^{-1}$ bands, indicating that three equivalent NO submolecules are involved in these vibrational modes.[37] Following the $Fe(NO)_3$ molecule, these four bands are assigned to the symmetric and antisymmetric N−O and Co−NO stretching vibrations of the $Co(NO)_3$ molecule with $C_{3v}$ symmetry. Again, the N−O stretching overtone bands were observed, at 3630.8 and 3530.9 $cm^{-1}$ ($A$ = 0.013 and 0.011); these bands are 1.6 $cm^{-1}$ *above* and 9.3 $cm^{-1}$ below the sum of fundamentals. The N−O stretching vibrations are shifted to 1825.6 and 1782.1 $cm^{-1}$ in solid neon, but the Co−NO stretching modes could not be observed due to noise caused by mechanical vibration of the 4 K cold machine. The assignments are strongly supported by DFT calculations, which predict a $^1A_1$ ground state with symmetric and antisymmetric N−O and Co−NO stretching vibrations at 1886.2, 1796.0, 595.2, and 531.7 $cm^{-1}$, which are in good agreement with experimental values. The compound $Co(NO)_3$ is of some interest as a closed-shell transition metal nitrosyl since the chromium compound $Cr(NO)_4$ is the only transition metal nitrosyl yet isolated.[24,39]

**Ni(NO)$_{1,2}$.** The NiNO molecule has been studied in detail very recently; the overtone and N−O and Ni−NO stretching vibrational modes were reported at 3324.3, 1677.1, and 608.4 $cm^{-1}$ in solid argon,[13] and the strongest band at 1676.2 $cm^{-1}$

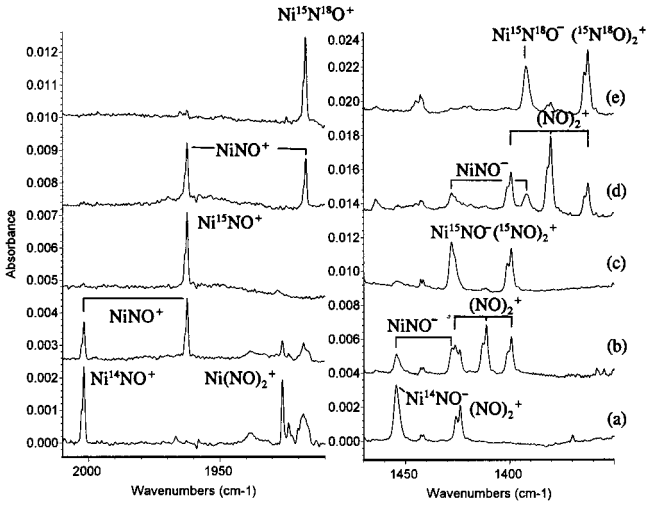


**Figure 10.** Infrared spectra in the 2010−1910 and 1470−1350 cm$^{-1}$ regions from co-deposition of laser-ablated nickel with isotopic NO in excess neon: (a) 0.1% $^{14}N^{16}O$, (b) 0.1% $^{14}N^{16}O$ + 0.1% $^{15}N^{16}O$, (c) 0.1% $^{15}N^{16}O$, (d) 0.1% $^{15}N^{16}O$ + $^{15}N^{18}O$, and (e) 0.1% $^{15}N^{18}O$.

was observed in the earlier work.[12] Similar bands at 3323.7, 1676.6, and 608.5 cm$^{-1}$ in our argon matrix experiments are assigned to the NiNO molecule. The 1676.6 and 608.5 cm$^{-1}$ bands are 30:1 relative absorbance. The resolved $^{58}$NiNO and $^{60}$NiNO bands at 608.5 and 605.2 cm$^{-1}$ clearly show that a single Ni atom is involved in this vibrational mode and molecular species. The overtone and N−O stretching vibration of NiNO are observed at 3331.5 and 1680.1 cm$^{-1}$ in our neon matrix. Our BP86 and B3LYP and earlier DFT calculations[12,13] predict a $^2$A′ ground state for NiNO with bond angle around 140°. The two modes were calculated at 1703.9 and 644.8 cm$^{-1}$ with BP86 with 42:1 relative intensity and at 1726.0 and 518.3 cm$^{-1}$ with B3LYP and 22:1 relative intensity.

Bands at 3555.2, 1749.7, 524.4, and 520.2 cm$^{-1}$ in argon matrix experiments increased on annealing. The weak 3555.2 cm$^{-1}$ band also shifted with $^{15}N^{16}O$ and $^{15}N^{18}O$ as expected for a N−O stretching mode. The 1749.7 cm$^{-1}$ band exhibited N−O stretching vibrational ratios, and triplets were presented in the mixed experiments. The 524.4 and 520.2 cm$^{-1}$ bands exhibited the intensity distribution appropriate for natural abundance $^{58}$Ni and $^{60}$Ni, clearly indicating one Ni atom involvement. These bands are assigned to the combination band of sym and antisym N−O stretching modes, and the antisymmetric N−O and Ni−NO stretching vibrations of the Ni(NO)$_2$ molecule. The difference 3555.2−1749.7 = 1805.5 cm$^{-1}$, with correction for anharmonicity, is reasonable for the symmetric N−O stretching mode. The N−O stretching combination and fundamental were observed at 3572.8 and 1759.9 cm$^{-1}$ in solid neon. BP86 calculation predicted a linear Ni(NO)$_2$ molecule to have a $^3\Sigma_g^-$ ground state with symmetric and antisymmetric N−O and Ni−NO stretching frequencies at 1848.7, 1777.3, and 533.8 cm$^{-1}$, which are in excellent agreement with observations.

The 1651.7 cm$^{-1}$ argon and 1660.4 cm$^{-1}$ neon matrix bands increase markedly on later annealings and appear to be due to a higher nitrosyl (NO)$_x$−NiNO with a single end-bonded nitrosyl weakly interacting with other inequivalent NO subunit(s).

**M-($\eta^2$-NO)**. Weak bands in the 1350−1250 cm$^{-1}$ region were observed in all three metal + NO reaction systems. These bands exhibited almost the same isotopic frequency ratios as the diatomic NO molecule, which indicates that these bands are due to N−O stretching vibrations. Since the frequencies are 500−600 cm$^{-1}$ lower than NO, side-bonded species must be considered following several examples in the Sc, V, and Cr systems.[24,26,27]

The 1343.8 and 1342.2 cm$^{-1}$ absorptions are assigned to the Fe−($\eta^2$-NO) molecule in solid argon and neon based on doublet isotopic structure in the mixed experiments. A band at 1347.2 cm$^{-1}$ in solid nitrogen assigned to Fe$^+$NO$^-$ is apparently the same species.[36] Our DFT calculations predicted a $^2$A′ ground state, in agreement with previous calculations,[21] which is 20.4 kcal/mol (BP86) higher in energy than $^2\Delta$ FeNO. The N−O stretching vibrational frequency is calculated at 1271.0 cm$^{-1}$ with BP86, which is lower than the observed value; apparently, other low-energy configurations contribute to the ground state of Fe−($\eta^2$-NO). The 1275.4 cm$^{-1}$ band with iron gave a broad doublet in the mixed $^{14}N^{16}O$ + $^{15}N^{16}O$ and $^{15}N^{16}O$ + $^{15}N^{18}O$ experiments, indicating slight perturbation from another NO, and a weak band at 1799.0 cm$^{-1}$ associated with the 1275.4 cm$^{-1}$ band, showed terminal N−O stretching vibrational frequency ratios. These two bands are assigned to the N−O stretching vibrations of the ON−Fe−($\eta^2$-NO) molecule.

The 1284.2 and 1317.4 cm$^{-1}$ absorptions are assigned to the Co−($\eta^2$-NO) molecule in solid argon and neon, respectively. This mode was calculated at 1341.8 (BP86) and 1394.5 cm$^{-1}$ (B3LYP) in its $^1$A′ ground state, which are 16.8 kcal/mol (BP86) and 13.2 kcal/mol (B3LYP) higher than the $^1\Sigma^+$ CoNO molecule.

The N−O stretching vibration of Ni−($\eta$-NO) is observed at 1293.7 cm$^{-1}$ in argon and 1292.6 cm$^{-1}$ in neon, which is in good agreement with the recently reported 1293.8 cm$^{-1}$ argon matrix value.[13] Present DFT calculations predict a $^2$A″ ground state for Ni−($\eta^2$-NO), which is 20.5 (BP86) and 11.6 kcal/mol (B3LYP) higher in energy than $^2$A′ NiNO molecule, with N−O stretching vibrational frequency at 1313.4 (BP86) and 1374.7 cm$^{-1}$ (B3LYP).

**MNO$^+$**. Weak bands were observed in the 2010−1890 cm$^{-1}$ region in neon matrix experiments for all three metal systems studied here: Fe 1897.3 cm$^{-1}$, Co 1957.5 cm$^{-1}$, and Ni 2001.9 cm$^{-1}$. These bands increased on lower temperature annealing and disappeared on full arc photolysis. The band positions are higher than the diatomic NO frequency at 1874.4 cm$^{-1}$ in neon and are enhanced in $CCl_4$ doping experiments on sample deposition, with respect to the MNO species, which strongly suggest cation assignments.[29,40] All these bands exhibit N−O stretching vibrational frequency ratios, and only pure isotopic counterparts are present in the mixed $^{14}N^{16}O$ + $^{15}N^{16}O$ and $^{15}N^{16}O$ + $^{15}N^{18}O$ spectra (Figure 10 for Ni). These three bands are assigned to the N−O stretching vibrations of the FeNO$^+$, CoNO$^+$, and NiNO$^+$ cations.

The cation assignments are further confirmed by DFT calculations. Thomas et al.[20] reported a detailed study on binding of NO to first-row transition metal cations and predicted a $^3\Delta$ ground state for FeNO$^+$, $^2\Delta$ ground state for CoNO$^+$, and $^1\Sigma^+$ state for NiNO$^+$. The same ground states are obtained using both BP86 and B3LYP functional calculations, and the N−O stretching frequencies were calculated at 1951.0 and 1970.0 cm$^{-1}$ for FeNO$^+$, 2009.6 and 2034.9 cm$^{-1}$ for CoNO$^+$, and 2043.2 and 2144.8 cm$^{-1}$ for NiNO$^+$, respectively, which are in good agreement with experimental values. The BP86 scale factors are 0.972, 0.974, and 0.980, respectively.

A previous ion cyclotron resonance mass spectrometric study on the reactivity of NO with Fe$^+$ reported that only metastable excited Fe$^+$ reacts with NO;[14] however, in our experiments, the FeNO$^+$ cation absorption increased on annealing (Figure 1). There are two possible routes to form FeNO$^+$ in our neon matrix: Fe$^+$ reaction with NO or Fe reaction with NO$^+$. Since

**TABLE 4: Calculated Geometries, Relative Energies (kcal/mol), Mulliken Charge Populations, and Dipole Moments (D) for $MNO^+$, MNO, and $MNO^-$ (M = Fe, Co, Ni)**

| | molecule | rel energy | geometry | M | N | O | D |
|---|---|---|---|---|---|---|---|
| BP86 | FeNO ($^2\Delta$) | 0 | Fe−N 1.593 Å<br>N−O 1.186 Å<br>linear | +0.25 | −0.21 | −0.04 | 3.5 |
| | Fe−($\eta^2$-NO)($^2$A″) | +20.4 | Fe−N 1.703 Å<br>N−O 1.268 Å<br>Fe−O 1.964 Å | +0.21 | −0.11 | −0.10 | 3.5 |
| | Fe−($\eta^2$-NO)($^2$A′) | +27.1 | Fe−N 1.705 Å<br>N−O 1.285 Å<br>Fe−O 1.918 Å | +0.42 | −0.17 | −0.25 | 3.3 |
| | $FeNO^+$ ($^3\Delta$) | +171.8 | Fe−N 1.668 Å<br>N−O 1.151 Å<br>linear | +0.81 | −0.01 | +0.19 | 3.7 |
| | $FeNO^-$ ($^3$A′) | −29.1 | Fe−N 1.646 Å<br>N−O 1.224 Å<br>∠FeNO 158.6° | −0.56 | −0.24 | −0.20 | 2.2 |
| | CoNO ($^1\Sigma^+$) | 0 | Co−N 1.569 Å<br>N−O 1.182 Å<br>linear | +0.22 | −0.18 | −0.04 | 3.5 |
| | CoNO ($^3$A″) | +6.3 | Co−N 1.675 Å<br>N−O 1.190 Å<br>∠CoNO 141.4° | +0.09 | −0.12 | +0.03 | 1.6 |
| | Co−($\eta^2$-NO)($^1$A′) | +16.8 | Co−N 1.669 Å<br>N−O 1.253 Å<br>Co−O 1.906 Å | +0.16 | −0.09 | −0.07 | 3.1 |
| | $CoNO^+$ ($^2\Delta$) | +178.0 | Co−N 1.649 Å<br>N−O 1.140 Å<br>linear | +0.74 | +0.03 | +0.23 | 2.6 |
| | $CoNO^-$ ($^2$A′) | −24.6 | Co−N 1.598 Å<br>N−O 1.217 Å<br>∠CoNO 161.4° | −0.54 | −0.28 | −0.19 | 2.3 |
| | $CoNO^-$ ($^4$A″) | −18.2 | Co−N 1.685 Å<br>N−O 1.233 Å<br>∠CoNO 153.7° | −0.57 | −0.24 | −0.20 | 0.9 |
| | NiNO ($^2$A′) | 0 | Ni−N 1.665 Å<br>N−O 1.187 Å<br>∠NiNO 140.2° | +0.06 | −0.10 | +0.04 | 1.7 |
| | Ni−($\eta^2$-NO)($^2$A″) | +20.5 | Ni−N 1.783 Å<br>N−O 1.271 Å<br>Co−O 1.891 Å | +0.22 | −0.17 | −0.05 | 3.9 |
| | $NiNO^+$ ($^1\Sigma^+$) | +172.9 | Ni−N 1.637 Å<br>N−O 1.134 Å<br>linear | +0.65 | +0.10 | +0.25 | 1.8 |
| | $NiNO^-$ ($^1$A′) | −28.5 | Ni−N 1.702 Å<br>N−O 1.228 Å<br>∠NiNO 125.9° | −0.58 | −0.30 | −0.12 | 2.0 |
| | $NiNO^-$ ($^3$A″) | −22.7 | Ni−N 1.675 Å<br>N−O 1.233 Å<br>∠NiNO 149.3° | −0.55 | −0.27 | −0.18 | 0.8 |
| B3LYP | FeNO ($^2\Delta$) | 0 | Fe−N 1.702 Å<br>N−O 1.184 Å<br>linear | +0.30 | −0.26 | −0.04 | 3.4 |
| | Fe−($\eta^2$-NO)($^2$A′) | +21.0 | Fe−N 1.849 Å<br>N−O 1.273 Å<br>Fe−O 1.950 Å | +0.40 | −0.27 | −0.13 | 5.1 |
| | $FeNO^+$ ($^3\Delta$) | +166.9 | Fe−N 1.721 Å<br>N−O 1.146 Å<br>linear | +0.90 | −0.06 | +0.16 | 4.4 |
| | $FeNO^-$ ($^3$A′) | −32.1 | Fe−N 1.818 Å<br>N−O 1.217 Å<br>∠FeNO 152.7° | −0.52 | −0.30 | −0.18 | 2.1 |
| | CoNO ($^1\Sigma^+$) | 0 | Co−N 1.560 Å<br>N−O 1.172 Å<br>linear | +0.31 | −0.21 | −0.10 | 4.0 |
| | CoNO ($^3$A″) | −7.6 | Co−N 1.757 Å<br>N−O 1.183 Å<br>∠CoNO 136.3° | +0.13 | −0.13 | 0.00 | 1.4 |
| | Co−($\eta^2$-NO)($^1$A′) | +13.2 | Co−N 1.658 Å<br>N−O 1.240 Å<br>Co−O 1.890 Å | +0.23 | −0.11 | −0.12 | 3.6 |
| | $CoNO^+$ ($^2\Delta$) | +159.2 | Co−N 1.689 Å<br>N−O 1.134 Å<br>linear | +0.82 | −0.01 | +0.19 | 3.2 |

**TABLE 4: (Continued)**

| molecule | rel energy | geometry | M | N | O | D |
|---|---|---|---|---|---|---|
| $CoNO^-$ ($^2A'$) | −34.4 | Co−N 1.736 Å<br>N−O 1.214 Å<br>∠CoNO 178.1° | −0.43 | −0.39 | −0.18 | 1.8 |
| $CoNO^-$ ($^4A''$) | −34.1 | Co−N 1.745 Å<br>N−O 1.221 Å<br>∠CoNO 179.8° | −0.45 | −0.34 | −0.21 | 1.0 |
| NiNO ($^2A'$) | 0 | Ni−N 1.711 Å<br>N−O 1.182 Å<br>∠NiNO 138.2° | +0.16 | −0.16 | 0.00 | 2.7 |
| Ni−($\eta^2$-NO)($^2A''$) | +11.6 | Ni−N 1.830 Å<br>N−O 1.252 Å<br>Co−O 1.918 Å | +0.29 | −0.20 | −0.09 | 4.3 |
| $NiNO^+$ ($^1\Sigma^+$) | +173.5 | Ni−N 1.637 Å<br>N−O 1.117 Å<br>linear | +0.70 | +0.09 | +0.21 | 1.7 |
| $NiNO^-$ ($^1A'$) | −21.2 | Ni−N 1.692 Å<br>N−O 1.215 Å<br>∠NiNO 124.8° | −0.52 | −0.32 | −0.16 | 1.5 |

**TABLE 5: Calculated Vibrational Frequencies ($cm^{-1}$) and Intensities (km/mol) for the Structures Described in Table 4**

| | molecule | N−O | M−NO | MNO bending |
|---|---|---|---|---|
| BP86 | FeNO ($^2\Delta$) | 1785.7(714) | 657.7(1) | 307.9(22) |
| | Fe−($\eta^2$-NO)($^2A'$) | 1205.7(278) | 611.1(3) | 252.4(19) |
| | $FeNO^+$ ($^3\Delta$) | 1951.0(297) | 581.4(1) | 281.6(13) |
| | $FeNO^-$ ($^3A'$) | 1561.3(1066) | 570.6(20) | 220.5(46) |
| | CoNO ($^1\Sigma^+$) | 1832.0(503) | 704.5(9) | 302.9(26) |
| | CoNO ($^3A''$) | 1685.5(827) | 628.7(15) | 277.0(8) |
| | Co−($\eta^2$-NO)($^1A'$) | 1341.8(180) | 755.6(17) | 342.1(9) |
| | $CoNO^+$ ($^2\Delta$) | 2009.6(326) | 598.8(0) | 223.4(13) |
| | $CoNO^-$ ($^2A'$) | 1611.6(961) | 605.0(76) | 217.0(81) |
| | $CoNO^-$ ($^4A''$) | 1502.3(1034) | 575.9(47) | 244.2(40) |
| | NiNO ($^2A'$) | 1703.9(798) | 644.8(19) | 269.2(7) |
| | Ni−($\eta^2$-NO)($^2A''$) | 1313.4(82) | 569.2(3) | 353.6(6) |
| | $NiNO^+$ ($^1\Sigma^+$) | 2043.2(324) | 614.1(2) | 230.1(8) |
| | $NiNO^-$ ($^1A'$) | 1456.4(1070) | 652.1(72) | 307.8(8) |
| | $NiNO^-$ ($^3A''$) | 1504.3(1017) | 590.8(72) | 243.1(35) |
| B3LYP | FeNO ($^2\Delta$) | 1775.7(1102) | 481.6(0.1) | 173.9(1) |
| | Fe−($\eta^2$-NO)($^2A'$) | 1312.0(94) | 427.9(18) | 306.0(2) |
| | $FeNO^+$ ($^3\Delta$) | 1970.0(369) | 535.2(11) | 248.0(13) |
| | $FeNO^-$ ($^3A'$) | 1603.0(649) | 374.9(24) | 108.8(12) |
| | CoNO ($^1\Sigma^+$) | 1883.5(663) | 719.7(15) | 296.9(32) |
| | CoNO ($^3A''$) | 1700.5(968) | 347.6(12) | 187.8(7) |
| | Co−($\eta^2$-NO)($^1A'$) | 1394.5(266) | 769.1(24) | 353.9(12) |
| | $CoNO^+$ ($^2\Delta$) | 2034.9(439) | 528.4(9) | 197.6(12) |
| | $CoNO^-$ ($^2A'$) | 1647.9(414) | 402.4(54) | 49.7(20) |
| | $CoNO^-$ ($^4A''$) | 1570.5(849) | 425.4(31) | 62.1(16) |
| | NiNO ($^2A'$) | 1726.0(922) | 518.3(42) | 245.2(10) |
| | Ni−($\eta^2$-NO)($^2A''$) | 1374.7(151) | 470.9(4) | 324.6(4) |
| | $NiNO^+$ ($^1\Sigma^+$) | 2144.8(468) | 620.0(5) | 219.1(8) |
| | $NiNO^-$ ($^1A'$) | 1514.9(1377) | 666.0(79) | 305.0(10) |

no $NO^+$ absorption is observed in our experiments, we suggest that $FeNO^+$ is formed by the reaction of ground state $Fe^+$ with NO. Our reagents are completely relaxed in the cold neon matrix.

Weak bands at 1910.7 and 1902.7 $cm^{-1}$ in Co + NO/Ne experiments increased on annealing, and disappeared on photolysis, which may also be due to cation absorptions, although the mixed isotopic spectra are not clear as this region is complicated by NO absorptions. These bands grow more on higher temperature annealing than $CoNO^+$ and are tentatively assigned to the $Co(NO)_2^+$ and $Co(NO)_3^+$ cations. DFT calculations predicted a $^1A_1$ ground state for $Co(NO)_2^+$ with strong antisymmetric N−O vibration at 1930.6 $cm^{-1}$ and weak symmetric N−O stretching vibration at 2007.5 $cm^{-1}$. The $Co(NO)_3^+$ cation was calculated to have a $^2A_2''$ ground state with $D_{3h}$ symmetry, and antisymmetric N−O vibration at 1925.3 $cm^{-1}$.

A similar band at 1926.2 $cm^{-1}$ in Ni + NO/Ne experiments is assigned to the $Ni(NO)_2^+$ cation (Figure 10); a 1918.3 $cm^{-1}$ band is tentatively assigned to the $Ni(NO)_3^+$ cation based on annealing behavior. A triplet was observed at 1926.2, 1901.7, and 1890.4 $cm^{-1}$ in the $^{14}NO/^{15}NO$ experiment and the 1926.2 $cm^{-1}$ band was enhanced relative to $Ni(NO)_2$ with $CCl_4$ added, which supports the $Ni(NO)_2^+$ assignments. Our DFT calculations, which predicted a $^2B_1$ $Ni(NO)_2^+$ ground state with antisymmetric N−O stretching vibration at 1935.7 $cm^{-1}$ and a $^1A_1''$ $Ni(NO)_3^+$ with $D_{3h}$ symmetry and antisymmetric N−O stretching vibration at 1926.1 $cm^{-1}$, provide additional support.

**$MNO^-$**. Weak bands were also observed in the 1600−1400 $cm^{-1}$ region in neon matrix experiments for the Co and Ni systems. These bands share common behavior: they are destroyed on photolysis and do not reproduce on further annealing after photolysis and they are reduced to <10% of former yield on $CCl_4$ doping, so anion species must be considered.[29,40] A 1454.7 $cm^{-1}$ band in Ni + NO/Ne experiments decreased on annealing, and shifted to 1428.2 $cm^{-1}$ using $^{15}N^{16}O$ sample and to 1392.1 $cm^{-1}$ using $^{15}N^{18}O$ sample. As shown in Figure 10, only pure isotopic counterparts are present in both mixed $^{14}N^{16}O + {}^{15}N^{16}O$ and $^{15}N^{16}O + {}^{15}N^{18}O$ spectra. Accordingly, the 1454.7 $cm^{-1}$ band is assigned to the N−O stretching vibration of the $NiNO^-$ anion. DFT calculations predicted a bent $^1A'$ ground state with N−O stretching vibration at 1456.4 $cm^{-1}$ (BP86) and 1514.9 $cm^{-1}$ (B3LYP). A weak band at 1592.2 $cm^{-1}$ is also due to an anion species; it shifted to 1559.1 and 1524.2 $cm^{-1}$ with $^{15}N^{16}O$ and $^{15}N^{18}O$ samples, and triplets with intermediates at 1571.2 and 1539.1 $cm^{-1}$ were observed in the mixed $^{14}N^{16}O + {}^{15}N^{16}O$ and $^{15}N^{16}O + {}^{15}N^{18}O$ experiments. This band is assigned to the antisymmetric N−O stretching vibration of linear $Ni(NO)_2^-$ anion. Our BP86 calculation predicted $Ni(NO)_2^-$ anion to have a $^2\Pi_u$ ground state with antisymmetric N−O stretching vibrations at 1596.5 $cm^{-1}$ and symmetric N−O stretching vibration at 1647.9 $cm^{-1}$ with no intensity, which strongly supports the $Ni(NO)_2^-$ anion assignment.

Similar absorptions were found in the Co + NO/Ne experiments: two weak bands at 1585.7 and 1593.8 $cm^{-1}$ observed on sample deposition were destroyed on photolysis and eliminated on $CCl_4$ doping. Although the mixed isotopic spectra were complicated by strong $(NO)_2^+$ and $NO_2$ absorptions, these two bands exhibited slightly different annealing behavior: the 1585.7 $cm^{-1}$ band slightly decreased on annealing while the 1593.8 $cm^{-1}$ band slightly increased, and accordingly, we assign the 1585.7 $cm^{-1}$ band to $CoNO^-$ and the 1593.8 $cm^{-1}$ band to $Co(NO)_2^-$. Our DFT calculation predicted a $^2A'$ ground state

**TABLE 6: Calculated (BP86) Geometries, Relative Energies (kcal/mol), Symmetric and Antisymmetric N−O and M−NO Vibrational Frequencies ($cm^{-1}$), and Intensities (km/mol) for $M(NO)_2^+$, $M(NO)_2$, and $M(NO)_2^-$ (M = Fe, Co, Ni)**

| molecule | rel energy | geometry | sym-NO | asym-NO | sym-MN | asym-MN |
|---|---|---|---|---|---|---|
| $Fe(NO)_2$ ($^1A_1$) | 0 | 1.628 Å<br>1.182 Å<br>114°, 161° | 1825.6(265) | 1752.4(1207) | 686.8(1) | 700.7(0.4) |
| $Fe(NO)_2$ ($^3B_1$) | +10.5 | 1.671 Å<br>1.186 Å<br>130°, 170° | 1798.7(133) | 1732.2(1529) | 632.0(2) | 622.0(5) |
| $Fe(NO)_2^+$ ($^2A_1$) | +184.4 | 1.690 Å<br>1.150 Å<br>118°, 164° | 1964.0(116) | 1891.3(1190) | 638.2(0) | 601.8(12) |
| $Fe(NO)_2^-$ ($^2B_1$) | −34.3 | 1.636 Å<br>1.221 Å<br>126°, 164° | 1631.8(581) | 1585.1(1352) | 617.2(1) | 660.8(23) |
| $Fe(NO)_2^-$ ($^4B_1$) | −31.0 | 1.674 Å<br>1.223 Å<br>150°, 180° | 1617.3(156) | 1565.1(1809) | 571.5(26) | 590.9(32) |
| $Co(NO)_2$ ($^2B_1$) | 0 | 1.648 Å<br>1.179 Å<br>128°, 166° | 1836.7(151) | 1767.3(1430) | 590.4(0.1) | 612.7(3) |
| $Co(NO)_2^+$ ($^1A_1$) | +177.6 | 1.663 Å<br>1.142 Å<br>116°, 162° | 2007.5(128) | 1930.6(1173) | 640.7(0) | 627.8(28) |
| $Co(NO)_2^-$ ($^3B_1$) | −43.3 | 1.651 Å<br>1.219 Å<br>147°, 173° | 1651.5(207) | 1598.0(1622) | 549.8(2) | 598.6(44) |
| $Co(NO)_2^-$ ($^1A_1$) | −33.8 | 1.647 Å<br>1.220 Å<br>143°, 170° | 1647.9(187) | 1597.0(1596) | 561.8(10) | 636.3(44) |
| $Ni(NO)_2$ ($^3\Sigma_g^-$) | 0 | 1.685 Å<br>1.178 Å<br>linear | 1848.7(0) | 1777.3(1631) | 477.0(0) | 533.8(28) |
| $Ni(NO)_2$ ($^1A_1$) | +14.3 | 1.676 Å, 1.179 Å<br>154°, 178° | 1840.3(27) | 1771.9(1730) | 506.2(2) | 602.8(7) |
| $Ni(NO)_2^+$ ($^2B_1$) | +191.2 | 1.709 Å<br>1.142 Å<br>140°, 174° | 2010.9(41) | 1935.7(1546) | 491.2(1) | 505.8(1) |
| $Ni(NO)_2^-$ ($^2\Pi_u$) | −41.3 | 1.663 Å<br>1.222 Å<br>linear | 1647.9(0) | 1596.5(1757) | 498.3(0) | 613.6(105) |

**TABLE 7: Calculated (BP86) Geometries, Vibrational Frequencies ($cm^{-1}$), and Intensities (km/mol) for $M(NO)_3$ (M = Fe, Co, Ni)**

| molecule | frequency (intensity) |
|---|---|
| $Fe(NO)_3$[a] ($^2A_1$) | 1861.9 (54)($a_1$), 1775.0 (1400)(e), 641.4 (10)($a_1$), 625.6 (16)(e), 567.7 (38)(e), 537.5 (1)($a_1$) |
| $Fe(NO)_3^+$ [b] ($^1A_1$) | 1989.6 (62)($a_1$), 1898.0 (1193)(e), 667.4 (2)($a_1$), 598.6 (30)(e), 566.3 (29)(e), 553.6(0)($a_1$) |
| $Co(NO)_3$[c] ($^1A_1$) | 1886.2 (17)($a_1$), 1796.0 (1215)(e), 641.7 (3)(e), 595.2 (3)($a_1$), 547.3 (0.3)($a_1$), 531.7 (35)(e) |
| $Co(NO)_3^+$ [d] ($^2A_2''$) | 2011.5 (0)($a_1'$), 1925.3 (1295)(e′), 540.7 (58)(e′), 533.4 (8)(e′), 468.8 (0)($a_1'$), 411.8 (0.4)($a_2''$) |
| $Ni(NO)_3^+$ [e] ($^1A_1''$) | 2013.8 ($a_1'$), 1926.1 (1400)(e′), 534.4 (2)(e′), 497.8 ($a_1'$), 447.0 (24)(e′), 440.9 ($a_1''$) |

[a] $C_{3v}$ symmetry, Fe−N 1.679 Å, N−O 1.174 Å, ∠NFeN 116°, ∠FeNO 170°. [b] $C_{3v}$ symmetry, Fe−N 1.696 Å, N−O 1.146 Å, ∠NFeN 110°, ∠FeNO 165°. [c] $C_{3v}$ symmetry, Co−N 1.658 Å, N−O 1.176 Å, ∠NCoN 119°. [d] $D_{3h}$ symmetry, Co−N 1.706 Å, N−O 1.142 Å. [e] $D_{3h}$ symmetry, Ni−N 1.726 Å, N−O 1.143 Å.

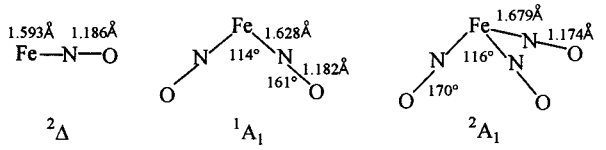


**Figure 11.** Structures calculated for iron nitrosyls using BP86/6-311+G*/Wachters−Hay.

for $CoNO^-$ anion, with N−O stretching vibrational frequency at 1611.6 $cm^{-1}$ (BP86) and 1647.9 $cm^{-1}$ (B3LYP). The same BP86 calculation found a $^3B_1$ ground state for $Co(NO)_2^-$ with antisymmetric and symmetric N−O stretching vibrations at 1598.0 and 1651.5 $cm^{-1}$.

There is no obvious evidence for the $FeNO^-$ and $Fe(NO)_2^-$ anions. Our DFT calculations predict that $FeNO^-$ anion has a $^3A'$ ground state with N−O stretching vibration at 1561.3 $cm^{-1}$ (BP86) and 1603.0 $cm^{-1}$ (B3LYP). In addition, $Fe(NO)_2^-$ was calculated to have a $^2B_1$ ground state with antisymmetric and symmetric N−O stretching vibrations at 1585.1 and 1631.8 $cm^{-1}$.

**Other Absorptions**. Since higher laser power was used in the argon experiments, the diatomic metal oxides were observed, and these molecules may also form complexes.[41−43] In Ni + NO/Ar experiments, bands at 1842.0, 883.5, and 879.4 $cm^{-1}$ were observed after deposition and slightly decreased on annealing. The upper band showed N−O stretching vibrational frequency ratios. The 883.5 and 879.4 $cm^{-1}$ bands exhibited intensity distribution appropriate for natural abundance $^{58}Ni$ and $^{60}Ni$; these two band have very little nitrogen-15 shift, but large oxygen-18 shift, and the 16/18 ratios (1.0413 and 1.0418) indicate a terminal Ni−O stretching vibration. The Ni isotopic shift 3.4 $cm^{-1}$ is larger than that of diatomic[42] NiO 825.6, 822.7 $cm^{-1}$, suggesting that the Ni atom is vibrating between two atoms. These bands are assigned to the ONiNO molecule.

**TABLE 8: Comparison of Observed (Neon and Argon) and Calculated (BP86) Vibrational Frequencies ($cm^{-1}$) and Scale Factors (Neon/Calculated) for Fe, Co, and Ni Nitrosyl Species**

| molecule | obsd (Ne) | obsd (Ar) | calcd | scale factor |
|---|---|---|---|---|
| $FeNO^+$ | 1897.3 | | 1951.0 | 0.972 |
| FeNO | 1766.0 | 1748.9 | 1785.7 | 0.989 |
| $Fe(NO)_2$ | 1810.8 | 1798.1 | 1825.6 | 0.992 |
| | 1744.6 | 1731.6 | 1752.4 | 0.996 |
| $Fe(NO)_3$ | 1757.8 | 1742.6 | 1775.0 | 0.990 |
| $Fe-(\eta^2\text{-NO})$ | 1342.2 | 1343.8 | 1271.0 | 1.056 |
| $CoNO^+$ | 1957.5 | | 2009.6 | 0.974 |
| CoNO | 1794.2 | 1761.0 | 1832.0 | 0.979 |
| $Co(NO)_2$ | 1749.1 | 1827.2 | 1836.7 | 0.990 |
| | | 1737.6 | 1767.3 | |
| $Co(NO)_3$ | 1825.6 | 1814.6 | 1886.2 | 0.968 |
| | 1782.1 | 1770.1 | 1796.0 | 0.992 |
| $Co-(\eta^2\text{-NO})$ | 1317.4 | 1284.2 | 1341.8 | 0.982 |
| $CoNO^-$ | 1585.7 | | 1611.6 | 0.984 |
| $Co(NO)_2^-$ | 1593.8 | | 1598.0 | 0.997 |
| $NiNO^+$ | 2001.9 | | 2043.2 | 0.980 |
| NiNO | 1680.1 | 1676.6 | 1703.9 | 0.986 |
| $Ni(NO)_2$ | 1762.0 | 1749.7 | 1777.3 | 0.991 |
| $Ni-(\eta^2\text{-NO})$ | 1292.6 | 1293.7 | 1313.4 | 0.984 |
| $NiNO^-$ | 1454.7 | | 1456.4 | 0.999 |
| $Ni(NO)_2^-$ | 1592.2 | | 1596.5 | 0.997 |

Similar bands at 1846.1 and 822.0 $cm^{-1}$ observed in Co + NO/Ar experiments are assigned to the N−O and Co−O stretching vibrations of the OCoNO molecule. The latter is below diatomic[43] CoO at 846.2 $cm^{-1}$.

Several weak bands in all three metal reaction systems increased on higher temperature annealing; these may arise from species that contain more than one metal atom and are simply labeled as $M_x(NO)_y$ in the tables. Finally, the only possible evidence for a NMO insertion product is the 942.7 $cm^{-1}$ band in the Fe/NO system. This is a mixed FeN, FeO mode, and the states are difficult to model by theory for NFeO,[21,36] as is the case for NMnO.[25] Hence, we cannot make a definitive assignment.

**Model for NO on Metal Surface and Catalyst Systems**. The $MNO^+$, $M(NO)_x$, and $M(NO)_x^-$ species observed here provide an indicator of the adsorbed state of catalytically active metallic species on the metal surface or in the bulk of oxides and zeolites. The MNO systems are very similar to MCO systems which have been discussed earlier.[40] As listed in Table 4, adding electrons to $MNO^+$ to form MNO and $MNO^-$ increases the N−O bond lengths in the series, and Mulliken charge distributions show an increase in negative charge on the NO, and a decrease in nitrosyl vibrational frequencies.

The chemistry of group VIII metals and their interaction with nitric oxide has been investigated extensively on zeolites and metal oxides where NO is a probe for assessing the adsorbed state of the active metallic species.[3−11] Unfortunately, assignments to specific nitrosyls are not straightforward and our work can help in this regard. Iron(II) zeolite spectra are characterized by a dominant band near 1880 $cm^{-1}$, which appears immediately after exposure to low NO pressure and is ascribed to a mononitrosyl species, and weaker bands near 1910 and 1810 $cm^{-1}$, which increase with more NO and have been identified first as dinitrosyl[4,6,9] and finally as trinitrosyl[7] on the basis of mixed $^{14}NO/^{15}NO$ isotopic spectra. The $FeNO^+$ and FeNO mononitrosyl frequencies are calculated as 1951.0 and 1785.7 $cm^{-1}$ (Table 5), and a like calculation (BP86/6-311+G*) for $FeNO^{2+}$ predicts a $^4\Sigma^-$ state, 535.6 kcal/mol above FeNO, with 1.799, 1.116 Å bond lengths, (+1.61, −0.06, +0.45) Mulliken charges, and 2123.0 $cm^{-1}$ (202 km/mol), 455.6(1), 272.8(8) frequencies. The present scale factor for $FeNO^+$ predicts isolated $FeNO^{2+}$ at 2064 $cm^{-1}$ to go with the observed $FeNO^+$ and FeNO at 1897 and 1766 $cm^{-1}$ in solid neon. Comparison with our data shows that the 1880 $cm^{-1}$ absorbing mononitrosyl $Fe^{II}(NO)$ involves iron cation with a local charge near +1 *but certainly not* +2. For ferrous cations on metal oxides, mononitrosyls absorbing near 1810 and 1750 $cm^{-1}$ have been observed.[5,6,8] Clearly, the 1810 $cm^{-1}$ absorption is due to an iron nitrosyl with *only a partial* positive charge, and the 1750 $cm^{-1}$ band is due to a reduced nearly neutral iron nitrosyl species.

It is clear from our spectra that $Fe(NO)_2$ and $Fe(NO)_3$ bands are close together; however, mixed isotopic spectra provide a definitive identification. The antisymmetic mode of $Fe(NO)_3$ on zeolite is higher than the corresponding frequency for the isolated neutral complex, which means that the metal center in the zeolite is partially oxidized. The DFT calculations for $Fe(NO)_3$ and $Fe(NO)_3^+$ suggest that the effective charge is intermediate between 0 and +1.

Infrared spectra of cobalt(II) zeolites exposed to NO exhibit bands close to 1900 and 1815 $cm^{-1}$, the exact band positions depending on the zeolite framework.[3,4,10a] These were attributed to the antisymmetric and symmetric N−O stretches of a dinitrosyl complex[10a] of $Co^{2+}$, but these assignments must be *reversed* and the angle recalculated as 147°, which is in better agreement with the present DFT angles for cobalt dinitrosyl species. An additional band at 1880 $cm^{-1}$ in the $Co^{II}X$ system has been assigned to the mononitrosyl complex of this ion.[3] These frequencies are intermediate between those observed for the neutral and +1 cation Co(NO) and $Co(NO)_2$ species presented in this study, and allow an estimate of the charge at the active cobalt center to be estimated. Plots of the NO frequency vs charge for both $Co(NO)^{+,0,-}$ and $Co(NO)_2^{+,0,-}$ show linear relationships in each case. The $^3\Delta$ state $CoNO^{2+}$ species is calculated at 2160 $cm^{-1}$, higher by 150 $cm^{-1}$ than $CoNO^+$. The 1880 and 1815 $cm^{-1}$ mononitrosyl and dinitrosyl absorptions quoted above yield effective charges of +0.4 and +0.5, respectively, at the cobalt centers. The consistency of these estimates and the linear plots obtained with both sets of data lend indirect support to the assignment of the 1902.7 $cm^{-1}$ band in the neon experiment to $Co(NO)_2^+$.

Finally, NO- and $Ni^{2+}$-exchanged zeolites gave a sharp, strong band at 1892 $cm^{-1}$, which was interpreted as $(Ni^+)(NO^+)$.[11] In the present neon matrix experiments, $NiNO^+$ at 2001.9 $cm^{-1}$ and NiNO at 1680.1 $cm^{-1}$ clearly bracket the 1892 $cm^{-1}$ Ni(NO)/zeolite absorption and suggest that the local charge is near +0.7 at the metal site.

## Conclusions

Laser-ablated iron, cobalt, and nickel atoms were reacted with NO molecules during condensation in excess neon and argon. The end-on bonded $Fe(NO)_{1-3}$, $Co(NO)_{1-3}$, $Ni(NO)_{1-2}$ nitrosyls and side-bonded $Fe-(\eta^2\text{-NO})$, $Co-(\eta^2\text{-NO})$, and $Ni-(\eta^2\text{-NO})$ species are formed during sample deposition or on annealing. No clear evidence is found for inserted NMO oxide−nitride molecules that dominated the early transition metal−NO systems,[24−27] which is characteristic of the lower valence, late transition metals.

The $FeNO^+$, $CoNO^+$, and $NiNO^+$ mononitrosyl cations are produced via metal cation reactions with NO, and the $Ni(NO)_{1,2}^-$ and $Co(NO)_{1,2}^-$ anions are formed by electron capture of neutral molecules. Laser ablation produces clean metal atom sources for matrix isolation and FTIR investigation. Laser ablation also provides metal cations and electrons, which made possible the first vibrational spectroscopic investigation of Fe, Co, and Ni

nitrosyl cations and anions. The matrix spectra of $MNO^+$ and MNO bracket absorptions for M(II)NO species on oxides and zeolites and clearly characterize *partial* local positive charges at the metal nitrosyl site.

Density functional theory calculations were employed to help identify these nitrosyl molecules, cations, and anions. Table 8 compares the scale factors (observed/calculated) for the N−O stretching vibrational modes of the observed species in neon using the BP86 functional. The scale factors range from 0.968 to 0.999 for all species except Fe−($\eta^2$-NO) where the difficult subject molecule probably has other low-energy configurations.[21] Calculations using the B3LYP functional gave slightly higher frequencies, as found in previous comparisons.[45] Of more importance, DFT calculations predicted isotopic frequencies and isotopic frequency ratios, which match very well the subtle differences in the observed ratios.

**Acknowledgment.** We gratefully acknowledge N.S.F. support for this research under grant no. CHE 97-00116 and helpful discussions with a A. Citra.

## References and Notes

(1) Fukuda, Y. *Surf. Sci.* **1981**, *104*, L234. Breitschafter, M. J.; Umbach, E.; Menzel, D. *Surf. Sci.* **1981**, *109*, 493.
(2) Avouris, Ph.; DiNardo, N. J.; Demuth, J. E. *J. Chem. Phys.* **1984**, *80*, 491. Odörfer, G.; Jaeger, R.; Illing, G.; Kuhlenbeck, H.; Freund, H.-J. *Surf. Sci.* **1990**, *233*, 44.
(3) Windhorst, K. A.; Lunsford, J. H. *J. Am. Chem. Soc.* **1975**, *97*, 1407. Lunsford, J. H.; Hutta, P. J.; Lin, M. J.; Windhorst, K. A. *Inorg. Chem.* **1978**, *17*, 606.
(4) Jermyn, J. W.; Johnson, T. J.; Vansant, E. F.; Lunsford, J. H. *J. Phys. Chem.* **1973**, *77*, 2964. Yuen, S.; Chen, Y.; Kubsh, J. E.; Dumesic, J. A.; Topsoe, N.; Topsoe, H. *J. Phys. Chem.* **1982**, *86*, 3022.
(5) King, D. L.; Peri, J. B. *J. Catal.* **1983**, *79*, 164.
(6) Sueiras, J. E.; Homs, N.; Ramirez de la Piscina, P.; Gracia, M.; Fierro, J. L. G. *J. Catal.* **1986**, *98*, 264. Rethwisch, D. G.; Dumesic, J. A. *J. Phys. Chem.* **1986**, *90*, 1625.
(7) Morrow, B. A.; Baraton, M. I.; Roustan, J. L. *J. Am. Chem. Soc.* **1987**, *109*, 7541.
(8) Johnston, C.; Jorgensen, N.; Rochester, C. H. *J. Chem. Soc. Faraday Trans.* **1988**, *84*, 2001.
(9) Aparicio, L. M.; Hall, W. K.; Fang, S. M.; Ulla, M. A.; Millman, W. S.; Dumesic, J. A. *J. Catal.* **1987**, *108*, 233.
(10) (a) Shen, G. C.; Shido, T.; Ichikawa, M. *J. Phys. Chem.* **1996**, *100*, 16947. (b) Chang, Y. F.; McCarty, J. G. *J. Catal.* **1998**, *178*, 408.
(11) Naccache, C.; Ben Taarit, Y. *J. Chem. Soc., Faraday Trans. 2* **1973**, 1475.
(12) Ruschel, G. K.; Nemetz, T. M.; Ball, D. W. *J. Mol. Struct.* **1996**, *384*, 101.
(13) Krim, L.; Manceron, L.; Alikhani, M. E. *J. Phys. Chem.* A **1999**, *103*, 2592.
(14) Oriedo, J. V. B.; Russell, D. H. *J. Am. Chem. Soc.* **1993**, *115*, 8381.
(15) Cassady, J. C.; Freiser, B. S. *J. Am. Chem. Soc.* **1985**, *107*, 1566.
(16) Khan, F. A.; Steele, D. L.; Armentrout, P. B. *J. Phys. Chem.* **1995**, *99*, 7819.
(17) Bauschlicher, C. W. Jr.; Bagus, P. S. *J. Chem. Phys.* **1984**, *80*, 944.
(18) Fenske, R. F.; Jensen, J. R. *J. Chem. Phys.* **1979**, *71*, 3374.
(19) Blanchet, C.; Duarte, H. A.; Salahub, D. R. *J. Chem. Phys.* **1997**, *106*, 8778.
(20) Thomas, J. L. C.; Bauschlicher, C. W. Jr.; Hall, M. B. *J. Phys. Chem.* A **1997**, *101*, 8530.
(21) Fiedler, A.; Iwata, S. *J. Phys. Chem.* A **1998**, *102*, 3618.
(22) Duarte, H. A.; Salahub, D. R. *J. Phys. Chem. B* **1997**, *101*, 7464.
(23) Martinez, A.; Jamorski, C.; Medina, G. *J. Phys. Chem. A* **1998**, *102*, 4643.
(24) Zhou, M. F.; Andrews, L. *J. Phys. Chem.* A **1998**, *102*, 7452 (Cr + NO); **1998**, *102*, 10025 (Nb, Ta + NO).
(25) Andrews, L.; Zhou, M. F.; Ball, D. W. *J. Phys. Chem. A* **1998**, *102*, 10041 (Mn + NO).
(26) Zhou, M. F.; Andrews, L. *J. Phys. Chem.* A **1999**, *103*, 478 (V + NO).
(27) Kushto, G. P.; Zhou, M. F.; Andrews, L.; Bauschlicher, C. W. Jr. *J. Phys. Chem.* A **1999**, *103*, 1115 (Sc, Ti + NO).
(28) Burkholder, T. R.; Andrews, L. *J. Chem. Phys.* **1991**, *95*, 8697.
(29) Andrews, L.; Zhou, M. F. *J. Chem. Phys.* **1999**, *111*, 6036.
(30) Jacox, M. E.; Thompson, W. E. *J. Chem. Phys.* **1990**, *93*, 7609.
(31) Frisch, M. J.; Trucks, G. W.; Schlegel, H. B.; Gill, P. M. W.; Johnson, B. G.; Robb, M. A.; Cheeseman, J. R.; Keith, T.; Petersson, G. A.; Montgomery, J. A.; Raghavachari, K.; Al-Laham, M. A.; Zakrzewski, V. G.; Ortiz, J. V.; Foresman, J. B.; Cioslowski, J.; Stefanov, B. B.; Nanayakkara, A.; Challacombe, M.; Peng, C. Y.; Ayala, P. Y.; Chen, W.; Wong, M. W.; Andres, J. L.; Replogle, E. S.; Gomperts, R.; Martin, R. L.; Fox, D. J.; Binkley, J. S.; Defrees, D. J.; Baker, J.; Stewart, J. P.; Head-Gordon, M.; Gonzalez, C.; Pople, J. A. *Gaussian 94*, Revision B.1; Gaussian, Inc.: Pittsburgh, PA, 1995.
(32) Perdew, J. P.; *Phys. Rev. B* **1986**, *33*, 8822. Becke, A. D. *J. Chem. Phys.* **1993**, *98*, 5648.
(33) Lee, C.; Yang, E.; Parr, R. G. *Phys. Rev. B* **1988**, *37*, 785.
(34) McLean, A. D.; Chandler, G. S. *J. Chem. Phys.* **1980**, *72*, 5639. Krishnan, R.; Binkley, J. S.; Seeger, R.; Pople, J. A. *J. Chem. Phys.* **1980**, *72*, 650.
(35) Wachters, H. J. H. *J. Chem. Phys.* **1970**, *52*, 1033. Hay, P. J. *J. Chem. Phys.* **1977**, 66, 4377.
(36) Andrews, L.; Chertihin, G. V.; Citra, A.; Neurock, M. *J. Phys. Chem.* **1996**, 100, 11235.
(37) Darling, J. H.; Ogden, J. S. *J. Chem. Soc., Dalton Trans.* **1972**, 2496.
(38) Zhou, M. F.; Andrews, L. *J. Am. Chem. Soc.* **1998**, *120*, 11499.
(39) Swanson, B. I.; Satija, S. K. *J. Chem. Soc., Chem. Commun.* **1973**, 40.
(40) Zhou, M. F.; Andrews, L. *J. Am. Chem. Soc.* **1999**, *121*, 9171.
(41) Chertihin, G. V.; Saffel, W.; Yustein, J. T.; Andrews, L.; Ricca, A.; Bauschlicher, C. W. Jr. *J. Phys. Chem.* **1996**, *100*, 5261 (FeO) .
(42) Citra, A.; Chertihin, G. V.; Andrews, L.; Neurock, M. *J. Phys. Chem.* A **1997**, *101*, 3109 (NiO).
(43) Chertihin, G. V.; Citra, A.; Bauschlicher, C. W. Jr. *J. Phys. Chem. A* **1997**, *101*, 8793 (CoO).
(44) Zhou, M. F.; Andrews, L. *J. Phys. Chem. A* **2000**, *104*, 2618 (CuNO).
(45) Scott, A. P.; Radom, L. *J. Phys. Chem.* **1996**, *100*, 16502. Bytheway, I.; Wong, M. W. *Chem. Phys. Lett.* **1998**, *282*, 219.